

# Modified kagomé physics in the natural spin-1/2 kagomé lattice systems — kapellasite $\text{Cu}_3\text{Zn}(\text{OH})_6\text{Cl}_2$ and haydeeite $\text{Cu}_3\text{Mg}(\text{OH})_6\text{Cl}_2$

O. Janson,<sup>1</sup> J. Richter,<sup>2</sup> and H. Rosner<sup>1,\*</sup>

<sup>1</sup>*Max-Planck Institut für Chemische Physik fester Stoffe, D-01187 Dresden, Germany*

<sup>2</sup>*Institut für Theoretische Physik, Universität Magdeburg, D-39016 Magdeburg, Germany*

(Dated: June 21, 2024)

The recently discovered natural minerals  $\text{Cu}_3\text{Zn}(\text{OH})_6\text{Cl}_2$  and  $\text{Cu}_3\text{Mg}(\text{OH})_6\text{Cl}_2$  are spin 1/2 systems with an ideal kagomé geometry. Based on electronic structure calculations, we develop a realistic model which includes couplings across the kagomé hexagons beyond the original kagomé model that are intrinsic in real kagomé materials. Exact diagonalization studies for the derived model reveal a strong impact of these couplings on the magnetic ground state. Our predictions could be compared to and supplied with neutron scattering, thermodynamic and NMR data.

PACS numbers: 71.20.Ps, 75.30.Et, 91.60.Pn

Since decades, low-dimensional spin systems attract broad interest due to their intriguing, unusual ground states (GS) such as helically ordered, spin Peierls, spin-liquid or resonating valence-bond GS's [1, 2, 3, 4]. These unusual ground states are typically driven by competing interactions or geometric frustration. Two-dimensional (2D) quantum spin systems are of particular interest because the competition between quantum fluctuations and interactions seems to be well balanced, and fine tuning of this competition may lead to zero-temperature transitions between semi-classical and quantum phases [5]. There are several examples for strongly frustrated 2D quantum spin materials, e.g.  $\text{PbVO}_3$  [6] or  $\text{SrCu}_2(\text{BO}_3)_2$  [7], which can be well described by a frustrated spin-1/2 Heisenberg model. Such 2D quantum magnets are at present most suitable objects for the comparison between theory and experiment.

A simple but very challenging realization of a geometrically frustrated quantum magnet is the spin-1/2 Heisenberg antiferromagnet (HAFM) on a kagomé lattice. The kagomé HAFM attracts much interest due to its unusual classical and quantum GS's and low-temperature thermodynamics, see e.g. Refs. 8, 9, 10, 11, 12, 13, and also due to potential applications of a possible quantum spin-liquid state [14]. The recent discovery of a natural spin-1/2 kagomé compound  $\text{Cu}_3\text{Zn}(\text{OH})_6\text{Cl}_2$  (mineral herbertsmithite [15]) and a subsequent synthesis of good-quality samples [16] have spurred both experimental [17, 18] and theoretical [11, 12, 13] investigations of this frustrated magnetic system. The experimental results were quite unexpected: Curie-Weiss behavior with a rather large  $\Theta$ , an upturn in magnetic susceptibility at 75 K and no spin gap down to 100 mK are far from being consistently described by theory. The main obstacle for theoretical studies is the structural Cu—Zn disorder within this compound [19], which hampers the kagomé physics, but encourages the search for new materials. A very recent discovery of two isostructural spin-1/2 kagomé systems — the minerals kapellasite  $\text{Cu}_3\text{Zn}(\text{OH})_6\text{Cl}_2$  ([20], a metastable polymorph

of herbertsmithite) and haydeeite  $\text{Cu}_3\text{Mg}(\text{OH})_6\text{Cl}_2$  [21], widens the range of possible investigations. These systems are of great potential interest because (i) no cations are located between the planes, thus less coupling between kagomé layers is expected though the interlayer distance is reduced by about 1 Å (ii) the presence of two isostructural compounds should allow a systematic study of additional exchange couplings beyond the original kagomé model. We have performed a theoretical electronic structure study within density functional theory (DFT) and estimated the exchange parameters of a corresponding Heisenberg model. For this spin model we have calculated the classical GS and for a finite lattice of  $N = 36$  sites the quantum spin-1/2 GS.

The DFT calculations were performed using a full-potential nonorthogonal local-orbital scheme (FPLO version 6.00-24) [22] within the local density approximation (LDA). The Perdew and Wang parameterization of the exchange-correlation potential was chosen for the scalar relativistic calculations [23]. The default basis set was used. The strong on-site correlations of the Cu  $d$ -electrons were taken into account using the LSDA+ $U$  method [24]. Well converged  $k$ -meshes of 124 points for the conventional cell and 75 points for the supercell in the irreducible wedge were used.

The hexagonal crystal structure of both minerals consists of layers (Fig. 1) perpendicular to the  $c$  direction. These layers are built by a kagomé lattice of corner-sharing  $\text{CuO}_4$  plaquettes, which are tilted with respect to this plane, and  $\text{ZnO}_6$  (kapellasite) or  $\text{MgO}_6$  (haydeeite) octahedra bridging the “ring” of six  $\text{CuO}_4$  plaquettes. The Cu—O—Cu angle between two neighboring plaquettes is close to  $105^\circ$ , providing considerable ferromagnetic (FM) contributions to the exchange due to the vicinity to  $90^\circ$ . The kagomé layers are separated by Cl atoms, which are bonded to H atoms that stick out of the layers. The experimentally defined H position for haydeeite [25] yields the unusually short O—H distance of 0.78 Å, the H position in kapellasite has not been reported. To account for this structural peculiarity, the H position was relaxed

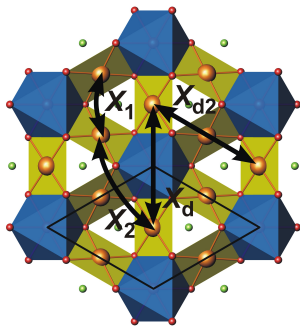


FIG. 1: (Color online) The hexagonal crystal structure of kapellasite and haydeeite:  $\text{CuO}_4$  plaquettes form a buckled kagomé layer bridged by  $\text{ZnO}_6/\text{MgO}_6$  octahedra. The inter-layer space is filled with Cl and H (not shown) atoms.

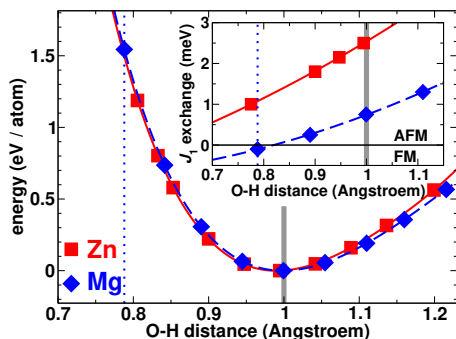


FIG. 2: (Color online) Total energy per H atom given by LDA calculations for kapellasite (Zn) and haydeeite (Mg). The zero energy corresponds to the calculated equilibrium distance and is marked with a gray line. The experimental value of the O—H distance in haydeeite is shown with a dotted line. Inset: exchange  $J_1$  from the supercell LSDA+ $U$  calculations as a function of the O—H distance.

with respect to the total energy, we show below that it has a dramatic impact on the exchange. Throughout the paper, we use the optimized H position [31] yielding  $\sim 1.0$  Å for the O—H distance (Fig. 2).

Our LDA calculations yield a valence band with a total width of 6—7 eV for both compounds with three bands crossing the Fermi level  $\varepsilon_F$  according to the three Cu atoms per unit cell (Fig. 3). The valence bands of haydeeite and kapellasite have two pronounced differences: (1) the rather localized  $d$ -states of Zn (between  $-6.5$  and  $-4$  eV) contribute to the valence band of kapellasite while Mg states have negligible contribution for haydeeite and (2) the width of the separated band complex at  $\varepsilon_F$  is slightly different. Nevertheless, the same model can be applied for the description of low energy excitations.

The band structure (Fig. 3) reveals that the dispersion perpendicular to the kagomé planes (along  $\Gamma$ —A) is very small, pointing to a pronounced 2D character of the systems in accordance with our expectations. The presence of states at Fermi level yields a metallic GS, contrary to the insulating behavior typical for undoped cuprates [32].

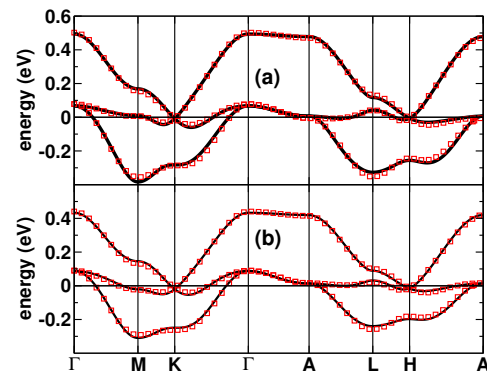


FIG. 3: (Color online) Band structures (solid lines) of kapellasite (a) and haydeeite (b) fitted to the TB model (squares).

This discrepancy originates from the strong on-site correlations of the Cu  $3d$  electrons, insufficiently described by LDA, and can be accounted for by adding the missing Coulomb repulsion in a model Hamiltonian or in the LSDA+ $U$  approximation. Though LDA fails to describe the electronic structure correctly, it can be used for an analysis of the magnetic excitations. To define the relevant orbitals for the low energy excitations we analyzed the density of states (DOS) by applying local coordinate systems for all orientations of  $\text{CuO}_4$  plaquettes and calculated the local DOS and band weights. The analysis revealed that the bands at Fermi level belong to local Cu  $3d_{x^2-y^2}$  and O  $2p_\sigma$  orbitals [33], i.e. the standard cuprate scenario with a half-filled antibonding  $dp\sigma^*$  band is realized. Therefore, an effective one-band model, already successfully applied for similar materials [26, 27], is appropriate to describe the magnetic excitations in these systems.

Three  $dp\sigma^*$  bands per unit cell lead to a  $3 \times 3$  matrix representing the tight-binding (TB) Hamiltonian. The number of transfer integrals, included into the TB model was picked to get a good fit of the LDA bands which could not be considerably improved by inclusion of further parameters. The fits shown in Fig. 3 were achieved using ten transfer integrals, though only four of them (Fig. 1) were larger than 10 meV. To check the stability of the leading terms, we subsequently decreased the number of parameters in our model. Basing on these results, we estimate less than 10% uncertainty in our values for the leading four transfer integrals depending on the chosen TB Hamiltonian. Thus, we can restrict ourselves to analysis of the leading terms. In order to estimate the antiferromagnetic (AF) exchange, the transfer integrals were mapped to an extended Hubbard model and subsequently to a Heisenberg model with  $J_i^{AF} = 4t_i^2/U_{eff}$  [34].

The leading AF exchange in both systems is the nearest-neighbor (NN) exchange  $J_1^{AF}$ , the second largest is the exchange along diagonals of a kagomé lattice,  $J_d^{AF}$  (see Fig. 1). The relevance of the latter exchange is rather unexpected: while the pure kagomé model includes  $J_1$

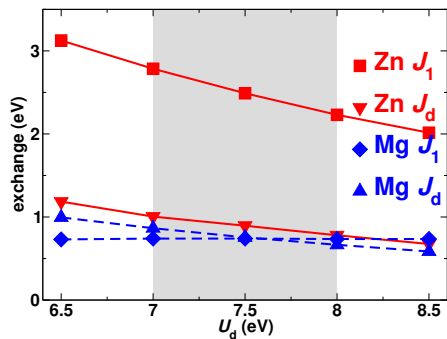


FIG. 4: (Color online) Exchange integrals of kapellasite and haydeeite as a function of Coulomb repulsion  $U$ .

path	kapellasite				haydeeite			
	$t$	$J^{AF}$	$J^{FM}$	$J$	$t$	$J^{FM}$	$J^{FM}$	$J$
$X_1$	87	7.5	-5.0	2.5	73	5.3	-4.5	0.8
$X_2$	-10	0.1	$\sim 0$	$< 0.1$	-9	0.1	$\sim 0$	$< 0.1$
$X_d$	49	2.4	-1.5	0.9	42	1.8	-1.0	0.8
$X_{d2}$	20	0.4	-0.4	$< 0.1$	22	0.5	-0.5	$< 0.1$

TABLE I: Transfer and exchange integrals of kapellasite and haydeeite. All values are given in meV. The values of transfer integrals are taken from the TB model. The AF exchange is calculated via subsequent mapping the transfer integrals to the extended Hubbard and Heisenberg models. The total exchange is taken from LSDA+ $U$  total energy calculations of supercells.  $J^{FM}$  is the difference between  $J$  and  $J^{AF}$ .

only, its modifications usually contain only the second neighbor  $J_2$  [28]. In our case, we find  $J_2^{AF}$  (and also  $J_{d2}^{AF}$ ) smaller than 0.5 meV for both systems, thus these terms can be neglected in the following discussion. The inter-plane coupling is much smaller than 0.1 meV, showing that the systems are almost perfect 2D magnets. Therefore, a  $J_1$ - $J_d$  model should be appropriate to describe the magnetism in good approximation.

The values of the total exchange were obtained using total energy calculations for supercells with different spin arrangements, where the difference in the values of total energy originates only from spin degrees of freedom. To obtain the leading exchange integrals, we used a doubled cell with six Cu atoms. The supercell calculations were performed using the LSDA+ $U$  method treating the correlation on a mean field level. This approach is necessary due to the Cu—O—Cu bond angle  $\approx 105^\circ$  which leads to sizable FM contribution according to Goodenough-Kanamori-Anderson rules.

The results are given in Table I ( $J^{FM}$  was evaluated as the difference between the total  $J$  and  $J^{AF} = 4t^2/U_{eff}$ ). The FM contributions significantly modify the size of the relevant exchange integrals, but preserve their AF nature. Here, we introduce the ratio  $\alpha \equiv J_d/J_1$ , which is zero in the simple kagomé model and runs to infinity in case of

decoupled chains. Certainly,  $\alpha$  may depend on external parameters like the H position and the  $U$  value. The change in O—H distance drastically affects the  $J_1$  exchange (Fig. 2, inset) in both compounds, and especially in haydeeite, where it becomes FM when the O—H bond is shorter than 0.8 Å. Thus, further quantitative analysis is based on the empirical fact that total energy calculations provide in general rather precise atomic positions. An accurate experimental determination of the H position is highly desirable for an improvement. The influence of the Coulomb repulsion  $U$  on  $\alpha$  is much weaker and there are no drastic changes in verified region (Fig. 4):  $\alpha$  is very close to 0.36 for kapellasite and stays in the vicinity of unity for haydeeite for the whole range of  $U$  studied. While GS's for  $\alpha = 0$  and  $\alpha = \infty$  are relatively clear, the region in between is not studied. Therefore, we have performed full diagonalization studies in order to clarify the influence  $\alpha$  on the GS.

It is well known that the classical GS of the pure kagomé HAFM ( $\alpha = 0$ ) is highly degenerate [8, 9, 10]. The additional diagonal bond  $J_d$  reduces this degeneracy drastically and selects non-coplanar GS's with twelve magnetic sublattices [35] among the huge number of classical kagomé GS's. These classical GS's of the  $J_1$ - $J_d$  model are characterized by a perfect antiparallel (Néel) spin alignment along the chains formed by diagonal bonds  $J_d$  and by a  $120^\circ$  spin arrangement on each triangle formed by NN bonds  $J_1$ . As a result, every two spin-sublattices are Néel-like antiparallel to each other and these two sublattices are perpendicular to one other group of two Néel-like sublattices.

For the quantum model the GS and low-lying excitations have been calculated by Lanczos diagonalization for the finite lattice of  $N = 36$  considered previously in the literature for the pure kagomé HAFM. Note that this finite lattice fits to the magnetic structure of the classical GS. The calculated spin correlations  $\langle \mathbf{S}_0 \mathbf{S}_{\mathbf{R}} \rangle$  for the classical GS as well as for the quantum GS for  $\alpha = 0.36$  and  $\alpha = 1.0$  are shown in Fig. 5. For comparison we also show  $\langle \mathbf{S}_0 \mathbf{S}_{\mathbf{R}} \rangle$  for the pure kagomé system, i.e.  $J_d = 0$ . Obviously, the quantum GS spin correlation is drastically changed by  $J_d$ . While for  $J_d = 0$  the decay of the spin correlation function is extremely rapid, we find a well pronounced short-range order for  $\alpha = 0.36$  and  $\alpha = 1.0$  that corresponds to the classical magnetic structure. This leads to the conclusion that even in the quantum model the GS has a non-coplanar magnetic structure giving rise to enhanced chiral correlations. Moreover, it is obvious from Fig. 5 that the magnetic correlations along the chains built by  $J_d$  bonds (in Fig. 5 that is for  $R/R_{NN} = 2$  and 4) are strongest, indicating that the low-energy excitations might be  $S = 1/2$  spinons causing an effectively one-dimensional low-temperature physics as has been discussed previously for other 2D models such as the crossed-chain model [29] as well as for the anisotropic triangular lattice [30]. However, this issue

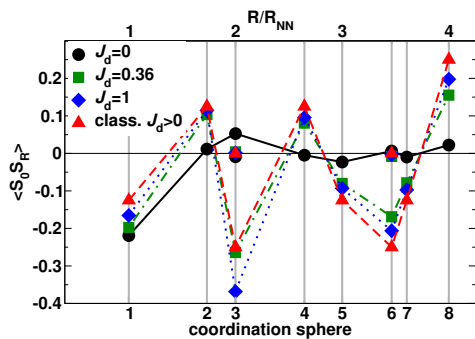


FIG. 5: (Color online) GS spin-spin correlation  $\langle \mathbf{S}_0 \mathbf{S}_{\mathbf{R}} \rangle$  versus separation  $R = |\mathbf{R}|$  for the  $J_1$ - $J_d$  HAFM on the kagomé lattice. The results for the quantum  $S = 1/2$  model are calculated for a finite lattice of  $N = 36$  sites. The lines are guides for the eyes connecting data points. Note that for  $R = 2$  and  $\sqrt{12}$  two non-equivalent spin-spin separations exist and the lines connect the points representing the stronger correlation.

needs further investigation.

Finally we mention another important difference from the pure kagomé system which is relevant for the low-temperature thermodynamics. For  $\alpha = 0$  the singlet-triplet gap (spingap) is filled by 210 non-magnetic excitations [11, 12] leading to different low-temperature behavior of the specific heat  $C$  (power-law in  $T$ ) and the susceptibility  $\chi$  (exponential decay). By contrast we find that for  $\alpha = 1$  ( $\alpha = 0.36$ ) there are no (only a few) singlets within the spingap. Therefore we do not expect any basic difference in the low- $T$  behavior of  $C$  and  $\chi$ .

To summarize, we have performed electronic structure calculations for two new spin-1/2 kagomé lattice compounds — kapellasite and haydeeite. Both compounds are 2D magnets, with two relevant AF exchanges: NN exchange  $J_1$  and the exchange along “diagonals” of a kagomé lattice  $J_d$ . We find  $\alpha \approx 0.36$  for kapellasite and  $\alpha \approx 1$  for haydeeite. The exchanges and thus  $\alpha$  values are strongly dependent on the H position for which the experimental value is unlikely with respect to the total energy and should be reinvestigated. The presence of significant  $J_d$  interaction leads to (i) non-coplanar magnetic order with 12 sublattices on the classical level which at least on a short-range scale, shows similarities to in the quantum model, and (ii) to the shift of the low-lying singlets out of the spingap. We especially emphasize the crucial importance of  $J_d$  for all real materials with kagomé geometry, which needs careful consideration in order to obtain the physically relevant model for the GS and the low lying excitations. This work is a starting point for study of these promising model compounds. Our predictions could be challenged and extended by neutron scattering, thermodynamic measurements,  $\mu$ SR and pressure experiments.

The work was supported by Emmy Noether program of DFG. We acknowledge fruitful discussions with S.-L. Drechsler and J. Schulenburg.

\* Electronic address: rosner@cpfs.mpg.de

- [1] R. Moessner, Can. J. Phys. **79**, 1283 (2001).
- [2] H. T. Diep, ed., *Frustrated Spin Systems* (World Scientific, 2004).
- [3] U. Schollwoeck, et al., eds., *Quantum Magnetism* (Springer, 2004).
- [4] R. Moessner and A. P. Ramirez, Physics Today **59** (2), 24 (2006).
- [5] S. Sachdev, Lect. Notes Phys. **645**, 381 (2004).
- [6] A. A. Tsirlin, et al., Phys. Rev. B **77**, 092402 (2008).
- [7] H. Kageyama, et al., Phys. Rev. Lett. **82**, 3168 (1999).
- [8] J. T. Chalker, P. C. W. Holdsworth, and E. F. Shender, Phys. Rev. Lett. **68**, 855 (1992).
- [9] D. A. Huse and A. D. Rutenberg, Phys. Rev. B **45**, 7536 (1992).
- [10] J. N. Reimers and A. J. Berlinsky, Phys. Rev. B **48**, 9539 (1993).
- [11] C. Waldtmann, et al., Eur. Phys. J. B **2**, 501 (1998).
- [12] C. Lhuillier, P. Sindzingre, and J.-B. Fouet, Can. J. Phys. **79**, 1525 (2001).
- [13] M. Rigol and R. R. P. Singh, Phys. Rev. Lett. **98**, 207204 (2007).
- [14] B. G. Levi, Physics Today **60** (2), 16 (2007).
- [15] R. S. W. Braithwaite, et al., Mineral. Mag. **68**, 527 (2004).
- [16] M. P. Shores, et al., J. Am. Chem. Soc. **127**, 13462 (2005).
- [17] P. Mendels, et al., Phys. Rev. Lett. **98**, 077204 (2007).
- [18] J. S. Helton, et al., Phys. Rev. Lett. **98**, 107204 (2007).
- [19] M. A. de Vries, et al., arXiv:0705.0654.
- [20] W. Krause, et al., Mineral. Mag. **70**, 329 (2006).
- [21] J. Schlüter and T. Malcherek, Neues Jahrbuch für Mineralogie — Abhandlungen **184**, 39 (2007).
- [22] K. Koepnik and H. Eschrig, Phys. Rev. B **59**, 1743 (1999).
- [23] J. P. Perdew and Y. Wang, Phys. Rev. B **45**, 13244 (1992).
- [24] H. Eschrig, K. Koepnik, and I. Chaplygin, J. Solid State Chem. **176**, 482 (2003).
- [25] T. Malcherek and J. Schlüter, Acta Cryst. B **63**, 157 (2007).
- [26] M. D. Johannes, et al., Phys. Rev. B **74**, 174435 (2006).
- [27] O. Janson, et al., Phys. Rev. B **76**, 115119 (2007).
- [28] J.-C. Domenge, et al., Phys. Rev. B **72**, 024433 (2005).
- [29] O. Starykh, R. Singh, and G. Levine, Phys. Rev. Lett. **88**, 167203 (2002).
- [30] R. Coldea, et al., Phys. Rev. Lett. **86**, 1335 (2001).
- [31] The crystal structures were determined by x-ray diffraction; this method usually does not allow to define the H position with good precision.
- [32] Blue transparent crystals evidence a gap of about 3 eV.
- [33] for “bridge” O atoms, connecting two Cu atoms, it is not possible to distinguish between  $p_\sigma$  contribution of one plaquette and  $p_z$  contribution of another.
- [34]  $U_{eff} = 4$  eV was used. Thus, the mapping is well justified in the strongly correlated limit  $U_{eff} \gg t_i$  at half-filling.
- [35] The GS’s are similar to the GS shown in Fig. 2 in Ref. 28.